Suppressive effects of Gua Lou Gui Zhi decoction on MCAO-induced NO and PGE_2 production are dependent on the MAPK and NF-κB signaling pathways

HAIXIA HU[1,2], XIAOQIN ZHU[1,2], RUHUI LIN[1,2], ZUANFANG LI[1,2] and LIDIAN CHEN[3]

[1]Academy of Integrative Medicine; [2]Fujian Key Laboratory of Integrative Medicine on Geriatrics; [3]College of Rehabilitation Medicine, Fujian University of Traditional Chinese Medicine, Fuzhou, Fujian 350108, P.R. China

Received September 29, 2015; Accepted October 7, 2016

DOI: 10.3892/mmr.2016.5876

Abstract. The present study aimed to investigate the inhibitory effects, and underlying mechanisms, of Gua Lou Gui Zhi decoction (GLGZD) in a rat model of neuroinflammation. Sprague-Dawley rats were treated with GLGZD following middle cerebral artery occlusion (MCAO). Neurological function and infarct volume were evaluated to confirm successful generation of the rat model. Subsequently, brain tissues and blood samples were collected for further analysis. Nitric oxide (NO) and prostaglandin E_2 (PGE_2) were evaluated in peripheral blood samples using the Griess reagent assay and an ELISA, respectively. The relative expression levels of inducible nitric oxide synthase (iNOS) and cylooxygenase-2 (COX-2) were detected by quantitative polymerase chain reaction and immunohistochemistry. The associated pathways, including nuclear factor-κB (NF-κB) and mitogen-activated protein kinases (MAPK) signaling pathways, were detected by electrophoretic mobility shift assay and western blotting. The results demonstrated that treatment with GLGZD significantly inhibited MCAO-induced inflammation; GLGZD suppressed the production of NO and PGE_2, and the expression of iNOS and COX-2, by inhibiting NF-κB activation and MAPK phosphorylation. These findings suggest that GLGZD, a potential agent for post-stroke treatment, may exert anti-inflammatory effects, thus providing neuroprotection.

Correspondence to: Professor Lidian Chen, College of Rehabilitation Medicine, Fujian University of Traditional Chinese Medicine, 1 Qiuyang Road, Minhou Shangjie, Fuzhou, Fujian 350108, P.R. China
E-mail: cld@fjtcm.edu.cn

Abbreviations: GLGZD, Gua Lou Gui Zhi decoction; MCAO, middle cerebral artery occlusion; NF-κB, nuclear factor-κB; MAPK, mitogen-activated protein kinases; NO, nitric oxide; iNOS, inducible nitric oxide synthase; PGE_2, prostaglandin E_2; ELISA, enzyme-linked immunosorbent assay; EMSA, electrophoretic mobility shift assay; ERK, extracellular signal-regulated kinase; GAPDH, glyceraldehyde 3-phosphate dehydrogenase; JNK, c-Jun N-terminal kinase; RT-qPCR, reverse transcription-quantitative polymerase chain reaction

Key words: GLGZD, nitric oxide, PGE_2, iNOS, cyclooxygenase-2, microglia, neuroinflammation

Introduction

Ischemic stroke is an acute vascular incident that occurs when blood supply to the brain is obstructed, resulting in irreversible brain damage. It has previously been reported that chronic microglial activation may lead to inflammation-mediated development of ischemic stroke, via the release of neurotoxic and inflammatory molecules (1). Overproduction of inflammatory mediators, such as nitric oxide (NO) and prostaglandin E_2 (PGE_2), from activated microglia may contribute to uncontrolled inflammation. Therefore, agents that inhibit activated microglia are important potential candidate drugs that may delay the progression of neurodegeneration in disorders such as stroke. Our previous study indicated that Gua Lou Gui Zhi decoction (GLGZD) inhibits the production of proinflammatory mediators *in vitro* and *vivo* via related signaling pathways (2,3). However, the mechanism via which GLGZD inhibits neuroinflammation and exerts its neuroprotective effects remain to be completely elucidated.

The present study measured NO production in a rat middle cerebral artery occlusion (MCAO) model of experimentally-induced ischemic brain damage. Behavioral defects and infarct volume were detected to confirm the generation of a successful model. Subsequently, the expression levels of inducible nitric oxide synthase (iNOS) and cylooxygenase-2 (COX-2) were detected by reverse transcription-quantitative polymerase chain reaction (RT-qPCR) and immunohistochemistry (IHC). In addition, the present study aimed to investigate the mechanisms by which GLGZD inhibits the production of proinflammatory mediators. The present study demonstrated that GLGZD significantly inhibited the excessive release of NO and PGE_2, and simultaneously attenuated the mRNA and protein expression levels of iNOS and COX-2. The underlying mechanisms were shown to be associated with inhibition of the phosphorylation of three members of the mitogen-activated protein kinases (MAPK) family: Extracellular signal-regulated kinase 1/2 (ERK1/2), p38 MAPK and c-Jun N-terminal kinase

(JNK), and of nuclear factor-κB (NF-κB) activation. These results indicated that GLGZD exerts anti-inflammatory effects and suppresses the expression of inflammatory mediators via the MAPK and NF-κB signaling pathways. Therefore, these molecular mechanisms may be exploited for the clinical treatment of ischemic stroke.

Materials and methods

Reagents and animals. 2,3,5-Triphenyltetrazolium chloride (TTC) was obtained from Sigma-Aldrich (Merck Millipore, Darmstadt, Germany). RT-qPCR reagents were purchased from Takara Bio, Inc. (Otsu, Japan). The PGE_2 ELISA kit (cat. no. PKGE004B) was purchased from R&D Systems, Inc. (Minneapolis, MN, USA). The primary polyclonal antibodies targeting iNOS (cat. no. sc-49055) and COX-2 (cat. no. sc-23983), and the secondary horseradish peroxidase (HRP)-conjugated immunoglobulin G antibody were obtained from Santa Cruz Biotechnology, Inc. (Dallas, TX, USA). Specific antibodies against ERK1/2 (cat. no. 9102), phosphorylated (p)-ERK1/2 (cat. no. 9101), p38 (cat. no. 9212), p-p38 (cat. no. 9211), JNK (cat. no. 9252), p-JNK (cat. no. 9251) and β-actin (cat. no. 4967) were purchased from Cell Signaling Technology, Inc. (Danvers, MA, USA).

Male Sprague-Dawley rats (weight, 200-250 g; age, 6 weeks) were purchased from Shanghai SLAC Laboratory Animal Co., Ltd. (Shanghai, China). The rats were maintained under specific-pathogen-free conditions, and were housed in a temperature- (21±1˚C) and humidity-controlled environment with a 12 h/12 h light/dark cycle and fed a standard rodent diet. The present study was conducted in accordance with the Animal Facility Guidelines of the University (Fujian University of Traditional Chinese Medicine, Fuzhou, China). All experiments were performed in a randomized manner. Rats were randomly distributed into three groups (n=15/group), as follows: Sham-operated group, MCAO model group and MCAO model + GLGZD treatment group (0.15 mg/kg, orally), in which rats were orally administered GLGZD daily for 7 days. The study was approved by the Institutional Animal Care and Use Committee of Fujian University of Traditional Chinese Medicine (Fuzhou, China).

Preparation of GLGZD extracts. Medicinal materials (*Trichosanthis radix*, *Ramulus cinnamomi*, *Paeonia lactiflora*, *Glycyrrhiza radix*, *Zingiber officinale Roscoe* and *Fructus jujubae*) were purchased from Guo Yi Tang Chinese Herbal Medicine Store (Fujian, China). GLGZD extract was prepared for treatment, according to a previously described method (4). Briefly, fresh GLGZD was washed three times with tap water to remove salt. The crude plant mixture was soaked in double-distilled water for 30 min, and was extracted twice for 2 h. The obtained solution was then filtered and concentrated in a rotary evaporator to a final concentration of 1.16 g/ml for further use (5).

MCAO model development. Rats were subjected to MCAO, according to a previously described method (5). Briefly, after anesthetizing with 10% chloral hydrate, the left common carotid artery and external carotid artery were exposed. A poly-L-lysine-coated monofilament nylon suture was inserted into the internal carotid artery for occlusion; the suture was maintained intraluminally for 2 h, after which it was withdrawn to restore cerebral blood flow. Finally, the chest cavity was closed and sutured. In the sham group, the MCO of rats was isolated without ligation and occlusion. Body temperature was monitored and maintained at 37˚C during the whole surgical procedure.

Behavioral testing. Neurological behavior in the groups was measured and scored according to a previously described method (6). Briefly, neurological deficits were assessed blindly at 2 h and 7 days post-reperfusion. The neurological function score ranged between 0 and 4, as follows: 0, Exhibition of normal, spontaneous movements; 1, unable to completely extend the right forepaw; 2, repetitive circling to the right; 3, unable to move to the right; 4, incapable of walking unimpeded.

TTC staining. Six rats from each of the three groups were decapitated following anesthesis with 10% chloral hydrate (0.3 ml/100 g) 7 days after MCAO, and coronal brain tissues were placed on ice and maintained at -80˚C. Subsequently, the tissues were sliced into 2-mm sections and were immediately stained with 1% TTC (20 g/l) at 37˚C for 30 min. Images of the staining were captured using a digital camera (Canon Oxus 950IS; Canon, Inc., Tokyo, Japan) and the infarcted areas of each section were measured using image analysis software (ImageJ 1.37; National Institutes of Health, Bethesda, MD, USA). Infarct volume was presented as the percentage of total brain volume that was damaged.

NO assay. Blood was collected from the abdominal aorta and was centrifuged at 1,625 x *g* for 20 min at room temperature, in order to obtain plasma for subsequent measurements. The concentration of NO was assessed by measuring the amount of accumulated nitrite, which is an indicator of NO production, using a colorimetric assay with Griess reaction, as previously described (7). Plasma (100 µl) from three rats from each group was mixed with the same volume of Griess reagent [0.1% N-(1-naphthyl)-ethylenediamine, 1% sulfanilamide in 5% phosphoric acid] in a 96-well microtiter plate. Absorbance values were determined at 540 nm using a microplate absorbance reader (BioTek Germany, Bad Friedrichshall, Germany). NO concentration was determined following generation of a sodium nitrite standard curve.

Determination of PGE_2 by ELISA. PGE_2 levels were measured in harvested plasma from each group (n=3) using an ELISA kit, according to the manufacturer's protocol. The concentration of PGE_2 was measured at an absorbance of 450 nm using a microplate reader.

Western blot analysis. The cortex was dissected and immersed in lysis buffer containing protease inhibitor (Roche Diagnostics GmbH, Mannheim, Germany) for 30 min on ice. Lysates were then centrifuged at 12,000 x *g* for 10 min at 4˚C and the supernatants were collected for analysis. Total protein concentrations were determined using the bicinchoninic acid (BCA) method. Equal amounts of protein (50 µg) were separated by 10% SDS-PAGE and were transferred to polyvinylidene

fluoride membranes (EMD Millipore, Billerica, MA, USA). Membranes were then incubated with blocking solution (5% non-fat milk) for 1 h at room temperature to block non-specific binding, and were probed with primary antibodies overnight at 4˚C, including the phosphorylated and total forms of ERK1/2, p38 MAPK and JNK, and β-actin (1:1,000). Subsequently, the membranes were incubated with HRP-conjugated secondary antibody for 1 h at room temperature. The protein immunoreactive bands were detected using an enhanced chemiluminescence reagent (RPN2132; GE Healthcare Bio-Sciences, Pittsburgh, PA, USA) and ChemiDoc XRS$^+$ System imaging system (Bio-Rad Laboratories, Inc., Hercules, CA, USA). The band intensity was normalized to the β-actin band and quantitative analysis was performed using ImageJ software.

RT-qPCR. Rats were anesthetized with 10% chloral hydrate (0.3 ml/100 g) and the brain cortex was removed for RNA isolation. Briefly, total RNA was extracted using TRIzol® reagent (Invitrogen; Thermo Fisher Scientific, Inc., Waltham, MA, USA). Total RNA (2 μg) was reverse transcribed to produce cDNA using the First Strand cDNA Synthesis kit (Takara Bio, Inc.) according to the manufacturer's instructions. qPCR was performed using a SYBR Green I qPCR kit (Takara Bio, Inc.) according to the manufacturer's protocol. The following primers were used for qPCR: iNOS, forward 5'-CCTCGTTCAGCTCACCTTCG-3', reverse 5'-GCCGCTCTCATCCAGAACCT-3'; COX-2, forward 5'-ACTGACTATGAAGACCTATG-3', reverse 5'-TTAATATACGGATTGGAAGT-3'; and GAPDH, forward 5'-TGGAGTCTACTGGCGTCTT-3' and reverse 5'-TGTCATATTTCTCGTGGTTCA-3'. Amplification was performed using Applied Biosystems Prism 7500 (7500 software v2.0.5; Applied Biosystems; Thermo Fisher Scientific, Inc.) with the following cycling conditions: Pre-denaturation at 95˚C for 30 sec, followed by 40 cycles at 95˚C for 5 sec and 60˚C for 30 sec, and final melt curve at 95˚C for 15 sec, 60˚C for 1 min, 95˚C for 15 sec. The results were analyzed using the $2^{-\Delta\Delta Cq}$ method (8). Quantitative gene expression levels were assessed relative to reference gene levels (GAPDH).

IHC. Rats were anesthetized with 10% chloral hydrate (0.3 ml/100 g) and perfused transcardially with saline and 4% paraformaldehyde. The brains were then dissected and fixed in 4% paraformaldehyde for 30 min. All tissues sections were transferred to graded ethanol (70, 80, 90, 95, 95 and 100% for 30 min each), then dehydrated tissues were cleared in xylene (30 min) and embedded in paraffin. Subsequently, tissues were cut into 5-μm coronal slices, and dried for 1 h at 60˚C, deparaffinized in xylene and rehydrated with an ethanol gradient (100, 95, 90, 85 and 75%), and washed twice in PBS. The sections were removed and incubated in 0.3% H_2O_2 for 10 min and washed in distilled water. Nonspecific binding of paraffin-embedded sections was blocked with goat serum, and the sections were then incubated with rat anti-iNOS and anti-COX-2 primary antibodies (1:500) overnight at 4˚C. After washing three times with PBS, the sections were exposed to secondary antibodies (1:200) for 30 min at room temperature and were visualized with diaminobenzidine. Images of each cerebral cortex section were acquired using a light microscope (Leica DMI4000B, Leica Microsystems GmbH, Wetzlar, Germany) at x200 magnification. Semi-quantitative analysis was conducted by determining the percentage of positively stained cells using ImageJ software.

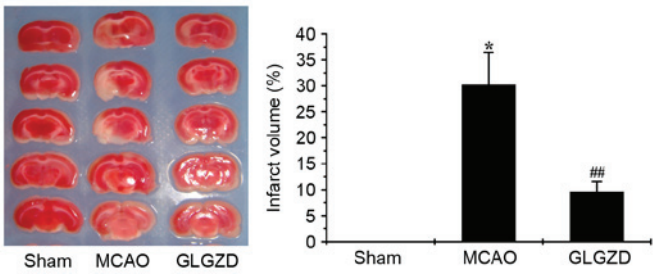

Figure 1. GLGZD decreased infarct volume, as detected by TTC staining. TTC-stained infarct volume was used to indicate the degree of ischemic brain damage. Red staining indicates healthy tissue, TTC does not stain infarcted areas. Compared with the MCAO group, GLGZD treatment significantly decreased infarct volume. Data are presented as the mean ± standard error of the mean (n=6). *P<0.05 vs. the sham group; $^{\#\#}$P<0.01 vs. the MCAO group. MCAO, middle cerebral artery occlusion; GLGZD, Gua Lou Gui Zhi decoction; TTC, 2,3,5-triphenyltetrazolium chloride.

Electrophoretic mobility shift assay (EMSA). Nuclear protein was extracted from the cerebral cortex for EMSA using a nuclear extraction kit (78833; Thermo Fisher Scientific, Inc.). Nuclear protein concentrations were determined using the BCA method (PICPI23223; Thermo Fisher Scientific, Inc.). EMSAs were performed using the EMSA/Gel-Shift kit (20148; Thermo Fisher Scientific, Inc.) according to the manufacturer's protocol. Briefly, a double-stranded biotin-labeled DNA oligonucleotide corresponding to the NF-κB p65 binding sequence (Cell Signaling Technology, Inc.; forward 5'-AGTTGAGGGGACTTTCCCAGGC-3' and reverse 3'-TCAACTCCCCTGAAAGGGTCCG-5') was used for gel shift assays. Nuclear protein (4.5 μg) from each sample was incubated with a biotin-labeled NF-κB probe for 30 min at room temperature, in a final volume of 20 μl. Subsequently, samples were subjected to nondenaturing gel electrophoresis (5% acrylamide, 0.5 X TBE) and were transferred to a nylon membrane (EMD Millipore) followed by crosslinked for 2 min. Finally, the membrane was visualized by chemiluminescence. Densitometry of the gel bands was analyzed using ImageJ software.

Statistical analysis. Data are presented as the mean ± standard error of the mean of three independent experiments. Statistical analysis was performed on SPPS 15.0 (SPSS, Inc., Chicago, IL, USA) using one-way analysis of variance and Dunnett's post-test. P<0.05 was considered to indicate a statistically significant difference.

Results

GLGZD reduces infarct volume in ischemic brain tissues. As shown in Fig. 1, the infarct volume was increased in the MCAO group compared with in the sham group. However, following GLGZD treatment for 7 days, ischemic infarction was significantly inhibited compared with in the MCAO group (P<0.01).

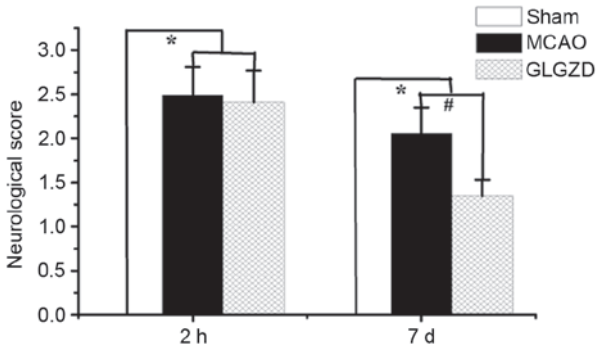

Figure 2. GLGZD reduced neurological behavioral scores following MCAO. Compared with the MCAO group, GLGZD treatment significantly improved neurological behavior, which was scored between 0 and 4. Data are presented as the mean ± standard error of the mean (n=8). *P<0.05 vs. the sham group; #P<0.05 vs. the MCAO group. MCAO, middle cerebral artery occlusion; GLGZD, Gua Lou Gui Zhi decoction.

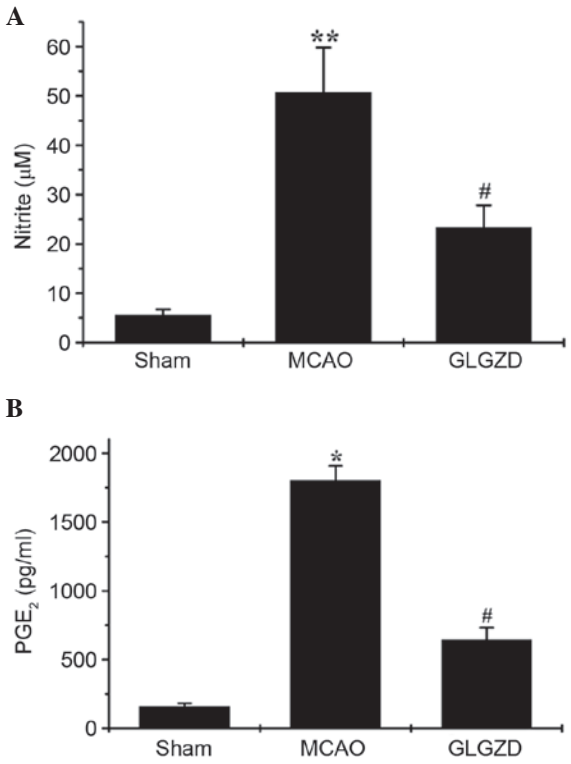

Figure 3. Inhibitory effects of GLGZD on MCAO-induced NO and PGE_2 release in rats. NO and PGE_2 production were measured by (A) Griess reaction and (B) ELISA, respectively. Administration of GLGZD significantly reduced the release of NO and PGE_2, which was markedly increased in the MCAO group. NO and PGE_2 release remained at basal levels in the sham group. Data are presented as the mean ± standard error of the mean from three independent experiments. *P<0.05, **P<0.01 vs. the sham group; #P<0.05 vs. the MCAO group. MCAO, middle cerebral artery occlusion; GLGZD, Gua Lou Gui Zhi decoction; NO, nitric oxide; PGE_2, prostaglandin E_2.

This result suggests that GLGZD exerts a therapeutic effect on ischemic brain tissue by decreasing cerebral infarction.

GLGZD improves the neurological deficit in an MCAO rat model. To determine the ameliorative effects of GLGZD on motor function, such as spasticity, in the postischemic brain, the present study evaluated neurological deficits 2 h and 7 days post-MCAO. Treatment with GLGZD markedly improved behavioral deficits caused by MCAO, and these deficits were not observed in the rats of the sham group (Fig. 2, P<0.05).

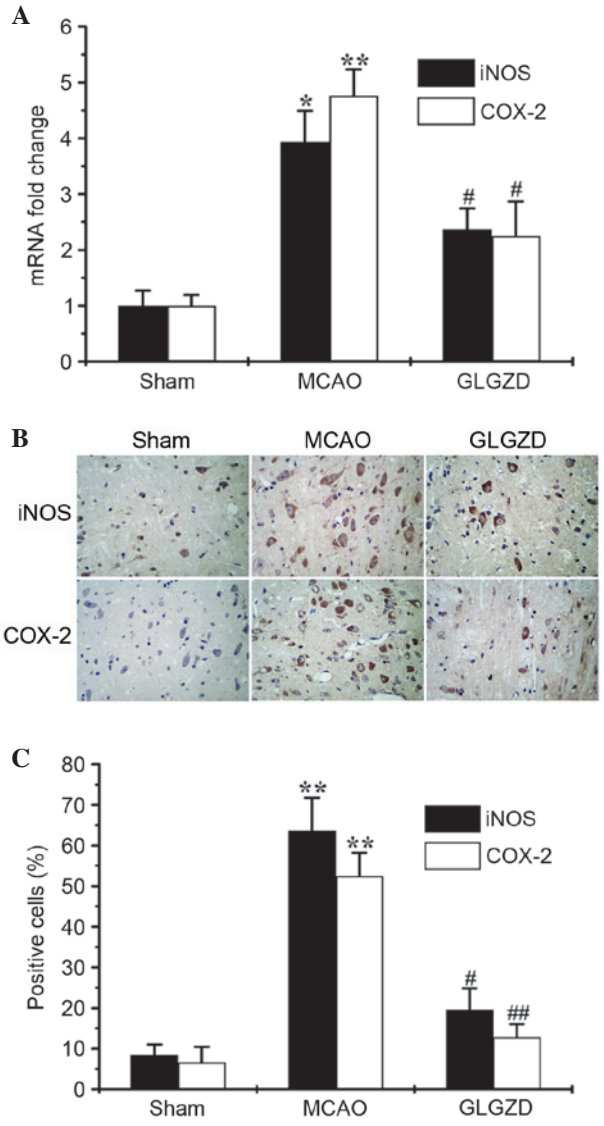

Figure 4. GLGZD attenuated the expression of iNOS and COX-2 in an MCAO rat model. (A) mRNA expression levels of iNOS and COX-2 were determined by quantitative polymerase chain reaction. GAPDH was used as an internal control. (B) Immunohistochemistry was performed to detect the corresponding protein levels of iNOS and COX-2. Images show representative results of the various groups from three independent experiments. (C) Semi-quantification of results from five randomly selected microscope fields (magnification, x200). Data are presented as the mean ± standard error of the mean from three independent experiments. *P<0.05, **P<0.01 vs. the sham group; #P<0.05, ##P<0.01 vs. the MCAO group. MCAO, middle cerebral artery occlusion; GLGZD, Gua Lou Gui Zhi decoction; iNOS, inducible nitric oxide synthase; COX-2, cylooxygenase-2.

GLGZD suppresses NO and PGE_2 release in plasma samples from the MCAO rat model. The effects of GLGZD on NO and PGE_2 production were investigated in all three groups using the Griess reagent assay and an ELISA, respectively. MCAO-induced elevation of NO and PGE_2 levels in the rats was significantly decreased following GLGZD administration (Fig. 3A and B, P<0.05). NO and PGE_2 release remained at basal levels in the sham group. These results indicate that

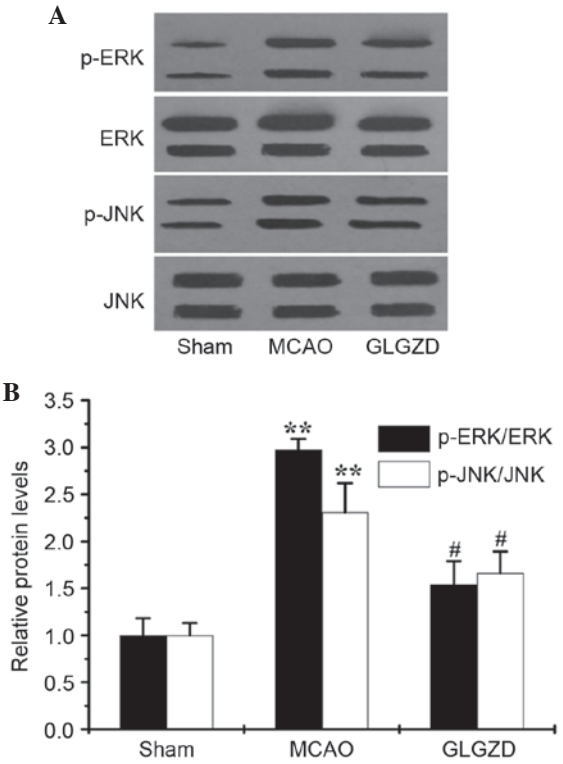

Figure 5. GLGZD suppressed the MAPK signaling pathway in an MCAO rat model. (A) Expression levels of p-MAPK molecules were analyzed by western-blotting. Image shows a representative immunoblot. (B) Semi-quantitative densitometric analysis of the p-/total-ERK1/2 and p-/total-JNK1/2 ratios was conducted. Data are presented as the mean ± standard error of the mean from three independent experiments. **P<0.01 vs. the sham group; $^{\#}$P<0.05 vs. the MCAO group. MCAO, middle cerebral artery occlusion; GLGZD, Gua Lou Gui Zhi decoction; MAPK, mitogen-activated protein kinase; p-, phosphorylated; ERK, extracellular signal-regulated kinase; JNK, c-Jun N-terminal kinase.

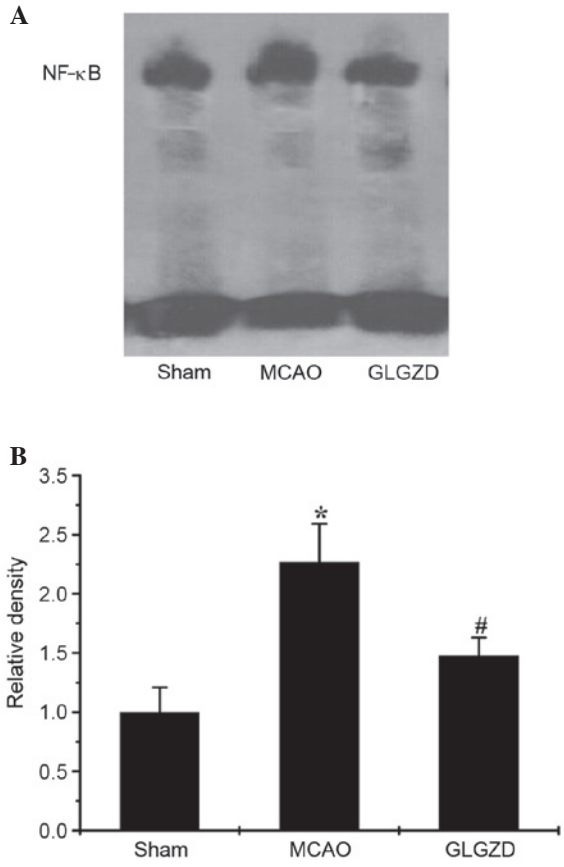

Figure 6. GLGZD decreased MCAO-induced NF-κB activation in a rat model. The effects of GLGZD on MCAO-induced activation of NF-κB were evaluated using electrophoretic mobility shift assay. (A) Image is representative of three independent experiments. (B) Quantification of NF-κB activation was presented as relative NF-κB binding activity. Data are presented as the mean ± standard error of the mean from three independent experiments. *P<0.05 vs. the sham group; $^{\#}$P<0.05 vs. the MCAO group. MCAO, middle cerebral artery occlusion; GLGZD, Gua Lou Gui Zhi decoction; NF-κB, nuclear factor-κB.

GLGZD exerts marked inhibitory effects on the production of proinflammatory mediators (NO and PGE_2).

GLGZD inhibits the mRNA and protein expression levels of iNOS and COX-2 in an MCAO model. It is well-known that NO is produced by iNOS, and PGE_2 is produced through induction of the proinflammatory enzyme COX-2 (9). The present study analyzed the expression levels of iNOS and COX-2 using qPCR and IHC. The results revealed that GLGZD significantly reduced iNOS and COX-2 transcriptional (Fig. 4A) and translational levels (Fig. 4B and C), which were increased in MCAO rats. The results of the IHC analysis of iNOS and COX-2 expression were consistent with those from the qPCR. These results indicate that treatment with GLGZD suppresses NO and PGE_2 production by inhibiting iNOS and COX-2 expression.

GLGZD downregulates phosphorylation of MAPKs and activation of NF-κB in an MCAO rat model. To examine whether GLGZD exerted inhibitory effects on proinflammatory mediators by regulating activation of the MAPK and NF-κB pathways, the phosphorylation of MAPKs (ERK1/2, JNK and p38 MAPK) were determined by western blot analysis, and NF-κB activity was detected by EMSA. Western blot analysis revealed that the levels of p-ERK1/2 and p-JNK, but not p-p38 MAPK, were enhanced in the MCAO group compared with the sham group (data not shown). However, treatment with GLGZD markedly reduced p-ERK1/2 and p-JNK levels in the ischemic brain (Fig. 5A and B), whereas total protein levels remained unchanged.

Following administration of GLGZD, NF-κB activation was also measured to determine the effects of GLGZD on the NF-κB pathway. As shown in Fig. 6A and B, a significant increase in the DNA-binding activity of NF-κB was observed in the MCAO group, as determined using an EMSA. Conversely, GLGZD markedly attenuated the DNA binding activity of NF-κB (P<0.05). These results suggest that signal transduction via MAPK and NF-κB is associated with neuroinflammation, and may be reduced by GLGZD in a rat model of cerebral ischemia.

Discussion

Neuroinflammation within the brain following stroke has been implicated in the pathogenesis of cerebral ischemia, and exacerbates secondary brain injury (10-12). Stroke induces an increase in the release of inflammatory mediators into the circulation. Microglia are innate immune cells in the central

nervous system, which serve a crucial role in neuroinflammation. Hyperactivated microglia produce large amounts of inflammatory molecules and promote neuronal death (13-15). Furthermore, microglial activation is correlated with sequential signaling pathways, including NF-κB and MAPK cascades, thus leading to the expression and production of proinflammatory mediators (16).

Among the inflammatory mediators released after ischemic stroke, released NO and PGE_2 from activated microglia serve an important role in the pathogenesis of neuroinflammation (17,18). NO is generated by iNOS (19) in microglial cells, and excessive production of NO produced from L-arginine by iNOS is detrimental (20). COX-2 is the key enzyme in the formation of PGE_2, which is produced by activated microglial cells and mediates neuropathological processes during neuroinflammation (21). Therefore, inhibition of inflammatory mediators that are responsible for the symptoms of neurodegenerative diseases is a potential therapeutic strategy for the treatment of neuroinflammation-associated ischemic stroke.

Various intracellular signaling pathways are involved in the modulation of neuroinflammatory mediators. The transcription factor NF-κB has a critical role in the inflammatory response to stroke (22). It has previously been reported that NF-κB activation can lead to the marked upregulation of iNOS and COX-2 (23-25). Furthermore, it has been reported that other signal transduction molecules, such as MAPK, are important upstream modulators for the production of inflammatory mediators (26). Therefore, the present study investigated the NF-κB and MAPK signaling pathways in order to clarify the underlying mechanism of GLGZD in neuroinflammation.

Our previous studies have revealed the neuroprotective effects of the traditional Chinese medicine GLGZD, and its effects have been suggested to have therapeutic potential for the treatment of spasticity following ischemic stroke (27,28). GLGZD is widely used in the treatment of spasticity after ischemic stroke in clinical practice. The present study examined the inhibitory effects of GLGZD on MCAO-induced production of proinflammatory mediators, including iNOS and COX-2, and the underlying mechanisms, including associated genes and signaling pathways.

As shown as the present study, infarct volume was markedly increased in the MCAO model group compared with in the sham group; however, it was decreased following treatment with GLGZD (Fig. 1, $P<0.01$). Similarly, GLGZD significantly alleviated the neurological deficit caused by MCAO (Fig. 2, $P<0.05$). In addition, GLGZD markedly inhibited MCAO-induced NO and PGE_2 production, as measured by Griess reagent assay and ELISA (Fig. 3A and B). Simultaneously, the relevant expression levels of iNOS and COX-2 were markedly increased in the MCAO model; however, treatment with GLGZD significantly reduced gene expression, as determined by RT-qPCR, and protein expression, as detected by IHC ($P<0.05$, Fig. 4A-C). To investigate the possible signal transduction mechanism associated with the inhibitory effects of GLGZD, the total and phosphorylated levels of the MAPK pathway proteins (ERK1/2, JNK and p38) were determined by western blotting. As presented in Fig. 5A and B, treatment with GLGZD attenuated the phosphorylation of ERK-1/2 and JNK, which was enhanced in MCAO rats ($P<0.05$); however, no influence was detected on p38 activation. The present study further explored the activation of NF-κB using EMSA; the results indicated that the NF-κB DNA-binding activity was significantly suppressed by GLGZD as compared with in the MCAO group (Fig. 6A and B, $P<0.01$). Taken together, these findings indicated that GLGZD may act as a potent inhibitor of MCAO-induced MAPK and NF-κB signaling.

In conclusion, the present study demonstrated that GLGZD exerted novel anti-inflammatory mechanisms in MCAO-mediated neuroinflammation. These results provide evidence of the ameliorative effects of GLGZD on NO and PGE_2 release and the suppression of related gene expression, including iNOS and COX-2, via the concomitant downregulation of MAPK and NF-κB signaling. Further studies are required to investigate the mechanism associated with the neuroprotective clinical effects of GLGZD.

Acknowledgements

The present study was supported by a grant from the National Natural Science Foundation of China (grant no. 81403265).

References

1. Brown GC and Neher JJ: Inflammatory neurodegeneration and mechanisms of microglial killing of neurons. Mol Neurobiol 41: 242-247, 2010.
2. Hu H, Li Z, Zhu X, Lin R, Lin J, Peng J, Tao J and Chen L: Gua Lou Gui Zhi decoction suppresses LPS-induced activation of the TLR4/NF-κB pathway in BV-2 murine microglial cells. Int J Mol Med 31: 1327-1332, 2013.
3. Hu H, Li Z, Zhu X, Lin R, Peng J, Tao J and Chen L: GuaLou GuiZhi decoction inhibits LPS-induced microglial cell motility through the MAPK signaling pathway. Int J Mol Med 32: 1281-1286, 2013.
4. Hu H, Lin R, Zhu X, Li Z and Chen L: Anti-inflammatory effects of Gualou Guizhi decoction in transient focal cerebral ischemic brains. Mol Med Rep 12: 1321-1327, 2015.
5. Huang J, Tao J, Xue X, Yang S, Han P, Lin Z, Xu W, Lin J, Peng J and Chen L: Gua Lou Gui Zhi decoction exerts neuroprotective effects on post-stroke spasticity via the modulation of glutamate levels and AMPA receptor expression. Int J Mol Med 31: 841-848, 2013.
6. Longa EZ, Weinstein PR, Carlson S and Cummins R: Reversible middle cerebral artery occlusion without craniectomy in rats. Stroke 20: 84-91, 1989.
7. Kovac A, Erickson MA and Banks WA: Brain microvascular pericytes are immunoactive in culture: Cytokine, chemokine, nitric oxide and LRP-1 expression in response to lipopolysaccharide. J Neuroinflammation 8: 139, 2011.
8. Livak KJ and Schmittgen TD: Analysis of relative gene expression data using real-time quantitative PCR and the 2(-Delta Delta C(T)) Method. Methods 25: 402-408, 2001.
9. Egger T, Schuligoi R, Wintersperger A, Amann R, Malle E and Sattler W: Vitamin E (alpha-tocopherol) attenuates cyclo-oxygenase 2 transcription and synthesis in immortalized murine BV-2 microglia. Biochem J 370:459-467, 2003.
10. Glezer I, Simard AR and Rivest S: Neuroprotective role of the innate immune system by microglia. Neuroscience 29: 867-883, 2007.
11. Perry VH, Nicoll JA and Holmes C: Microglia in neurodegenerative disease. Nat Rev Neurol 6: 193-201, 2010.
12. Rock RB and Peterson PK: Microglia as a pharmacological target in infectious and inflammatory diseases of the brain. J Neuroimmune Pharmacol 1: 117-126, 2006.
13. Minghetti L: Cyclooxygenase-2 (COX-2) in inflammatory and degenerative brain diseases. J Neuropathol Exp Neurol 63: 901-910, 2004.
14. Griffiths MR, Gasque P and Neal JW: The multiple roles of the innate immune system in the regulation of apoptosis and inflammation in the brain. J Neuropathol Exp Neurol 68: 217-226, 2009.
15. Amor S, Puentes F, Baker D and van der Valk P: Inflammation in neurodegenerative diseases. Immunology 129: 154-169, 2010.

16. Lo JY, Kamarudin MN, Hamdi OA, Awang K and Kadir HA: Curcumenol isolated from Curcuma zedoaria suppresses Akt-mediated NF-κB activation and p38 MAPK signaling pathway in LPS-stimulated BV-2 microglial cells. Food Funct 6: 3550-3559, 2015.
17. Banati RB, Gehrmann J, Schubert P and Kreutzberg GW: Cytotoxicity of microglia. Glia 7: 111-118, 1993.
18. Rock RB and Peterson PK: Microglia as a pharmacological target in infectious and inflammatory diseases of the brain. J Neuroimmune Pharmacol 1: 117-126, 2006.
19. Abramson SB, Amin AR, Clancy RM and Attur M: The role of nitric oxide in tissue destruction. Best Pract Res Clin Rheumatol 15: 831-845, 2001.
20. Boje KM: Nitric oxide neurotoxicity in neurodegenerative diseases. Front Biosci 9: 763-776, 2004.
21. Minghetti L: Cyclooxygenase-2 (COX-2) in inflammatory and degenerative brain diseases. J Neuropathol Exp Neurol 63: 901-910, 2004.
22. Harari OA and Liao JK: NF-κB and innate immunity in ischemic stroke. Ann N Y Acad Sci 1207: 32-40, 2010.
23. Baldwin AS Jr: The NF-kappa B and I kappa B proteins: New discoveries and insights. Annu Rev Immunol 14: 649-683, 1996.
24. Lee AK, Sung SH, Kim YC and Kim SG: Inhibition of lipopolysaccharide-inducible nitric oxide synthase, TNF-alpha and COX-2 expression by sauchinone effects on I-kappaBalpha phosphorylation, C/EBP and AP-1 activation. Br J Pharmacol 139: 11-20, 2003.
25. Baeuerle PA and Henkel T: Function and activation of NF-kappa B in the immune system. Annu Rev Immunol 12: 141-179, 1994.
26. Kim YJ, Hwang SY, Oh ES, Oh S and Han IO: IL-1beta, an immediate early protein secreted by activated microglia, induces iNOS/NO in C6 astrocytoma cells through p38 MAPK and NF-kappaB pathways. J Neurosci Res 84: 1037-1046, 2006.
27. Zhang L and Ai H: Effects of Gua Lou Gui Zhi decoction on c-fos and c-jun on epileptic Rats. Sichuan Journal of Traditional Chinese Medicine 23: 21-22, 2005.
28. Yang C, Chen L and Tao J: New usage of a classical formula-Gua Lou Gui Zhi Decoction. Liaoning Journal of Traditional Chinese Medicine 8: 166-167, 2012.